
Article:
Liu, Y., Huang, S.-S. orcid.org/0000-0003-2816-7104, Burgess, I. et al. (1 more author) (2024) Optimization of failure modes of a ductile connection under fire conditions. Fire Technology. ISSN 0015-2684

https://doi.org/10.1007/s10694-024-01571-3

Optimization of failure modes of a ductile connection under fire conditions

Yu Liu[1*], Shan-Shan Huang[2], Ian Burgess[2] and Bin Peng[1]

[1] School of Environment and Architecture, University of Shanghai for Science and Technology, Shanghai, 200093, China.

[2] Department of Civil and Structural Engineering, University of Sheffield, Mappin Street, Sheffield S1 3JD, United Kingdom.

*** Corresponding Author: E-mail address:** liuyu651020@usst.edu.cn

Abstract

Connections are the most vulnerable parts of a structure under fire conditions. A novel steel connection with high axial and rotational ductility has been proposed with the objective to improve the performance of steel-framed buildings in fire. Analytical model has been developed to determine the axial displacement of the top and bottom flanges of the beam end at high temperatures. A series of sub-frame models with this ductile connection have been built using Abaqus to study the influence of the characteristics of the connection part between the fin-plate part and face-plate part on the overall connection behaviour. The current critical failure mode of the ductile connection is bolt pull-out from the face-plate zone, and the tensile deformation capacity of the connection is not fully utilized. Therefore, measures to improve the bolt pull-out failure mode of the connection have been tested using the Abaqus sub-frame models, including adding a strengthening plate to the face-plate part of the connection and increasing the connection plate thickness. The simulation results show that the bearing failure of the beam web will become another critical failure mode of the connection, once the bolt pull-out failure is eliminated. To further optimize the high-temperature performance of the connection, the Abaqus steel frame models have also been used to test some measures to delay the occurrence of the beam web bearing failure, including adding strengthening plates to the part of the beam web in contact with the connection, and improving the material properties of the part of the beam web around the bolt holes at high temperatures.

Keywords: Fire; connections; ductility; failure mode, finite element modelling

Notation list

$\Delta_{low-temp,top}$	Axial ductility demand of the beam at the top flange at low temperatures
$\Delta_{low-temp,bottom}$	Axial ductility demand of the beam at the bottom flange at low temperatures
$\Delta_{high-temp,top}$	Axial ductility demand of the beam top flange at high temperatures
$\Delta_{high-temp,bottom}$	Axial ductility demand of the beam at the bottom flange at high temperatures
$\delta_{low-temp}$	Mid-span deflection of the beam at low temperatures
$\delta_{high-temp}$	Mid-span deflection of the beam under catenary action at high temperatures
$\theta_{low-temp}$	Beam end rotation at low temperatures
$\theta_{high-temp}$	Beam end rotation at high temperatures
l	The beam length
α	Thermal expansion coefficient
h	The height of the beam section
T	Beam temperature
ε_{total} / $\varepsilon_{thermal}$ / $\varepsilon_{mechanical}$	The total/ thermal/ mechanical strain of the beam section
E_T	Youngs modulus of steel at temperature T
Δ_C	The connection movement at high temperatures
r	The radius of the semi-cylindrical section
a	The semi-major axis of the semi-elliptical section
b	The semi-minor axis of the semi-elliptical section

1. Introduction

The collapse of buildings at the World Trade Centre in New York [1] and the Cardington full-scale fire tests [2] showed that connections are the most vulnerable structural elements of a steel building frame in a fire. Connection fractures may trigger the collapse of floors, buckling of columns, and eventually the disproportionate collapse of an entire building [3]. Connections are usually designed to carry forces under ambient-temperature loadings which are easily defined and calculated. However, in fire conditions, the deformation of the weakened connected beams causes a complex variation of forces and the generation of tying forces. During the initial heating stage, the beam applies axial compression to its connections due to restraint to free thermal expansion. Heating of the steel beam causes a free thermal expansion which, if stiffly restrained by surrounding structure such as protected columns, cooler beams, attached concrete slabs or braced bays, generates very

high axial compression. The net compression, hogging bending and shear near to the beam ends tend to cause localised shear buckling of the beam web and bottom flange buckling, which becomes more likely at relatively high temperature. If the free thermal expansion of the beam can be accommodated by soft, ductile surrounding structure, then the initial build-up of compressive force will be greatly reduced. As temperatures rise further, the net compression progressively reduces due to the sagging deflection of the beam and material degradation. At very high temperatures, the beam hangs, essentially in catenary tension, between its end connections, eventually deflecting just enough to balance its net tensile capacity against the catenary tension caused by its loading and deflection. When the beam is cooled from any peak temperature, its contraction as the material stiffens will generate high tensile forces between its ends. If the connections are ductile during this contraction phase, then this tension force can potentially also be reduced.

Researchers around the world have carried out comprehensive experimental and numerical studies on the high-temperature behaviour of different types of connections. Al-Jabri [4] conducted 20 high-temperature tests on flush and flexible end-plate joints, and studied the effects of several key parameters on joint performance. It was during the project that Al-Jabri realized that due to the lack of axial forces generated by the beam, the tests on isolated joints cannot reflect the real joint behaviour within a structural frame under fire conditions. Yu carried out a series of tests on web-cleat [5], fin-plate [6] and flush end-plate connections [7] at both room and elevated temperatures to study the failure modes of these three types of connections. It was found from the test results that flush end-plate connections exhibit much stiffer behaviour than fin-plate and web-cleat connections. Hu [8] found that compared with his test results, the tying capacities of the flexible end-plate connections calculated according to the Eurocode were overestimated. Huang [9] used the same test device as Yu and Hu to conduct a series of tests on reverse-channel connections, and found that the main failure modes of this type of connection include fracture of the reverse-channel web, punching failure and tensile fracture of bolts. Wang [10] conducted 10 high-temperature tests on restrained steel frames with different types of connections, and concluded that the influence of connection type should be taken into consideration if the beam catenary action is considered in fire resistant design. Song [11] applied cyclic load to welded steel joints under high temperatures to investigate the performance of joints in post-earthquake fire. The test results obtained by Sagiroglu [12] show that after fire, steel connections undergo large deformation under low load, and are more

prone to fracture.

Fire tests on connections are usually very expensive, and it is very difficult to reproduce the change of internal forces experienced by connections in real fire. Compared with experiments numerical simulation, which can consider the effects of degraded material properties, thermal expansion and combinations of forces, is a more feasible and economical method to study the connection behaviour under fire conditions. Several numerical approaches can be used, including simplified analytical models, curve-fit methods, detailed finite element modelling and component-based modelling. Sarraj [13, 14] used Abaqus models to carry out parametric studies on the fire performance of fin-plate connections considering the effects of geometric and material nonlinearity, large deformation and contact conditions. Yu [15] employed the dynamic-explicit solver in her Abaqus models to overcome convergence problems caused by the complex contacts within bolted steel connections, and the simulation results were in good agreement with the experimental results [4]. Qiang et al. [16] studied the fire behaviour of high-strength steel end-plate connections using Abaqus, and validated the moment-rotation curves, failure modes and yield-line patterns obtained from the simulation results against experimental results [17]. Rahnavard and Thomas [18] built Abaqus connection models to study the effect of fire on the performance of welded and bolted connections, and compared their numerical results with the experiments carried out by Wald [19] and Qiang [20]. Taib and Burgess [21] developed a component-based model of the fin-plate connection, based on the equations derived by Sarraj to calculate the characteristics of bolts in shear, fin-plate in bearing and beam web in bearing. Dong [22] proposed component-based models for end-plate connections and reverse-channel connections, and incorporated these two connection models into the software Vulcan. Lin [23] established the component-based model of the flexible end-plate connection which can consider the connection deformation after the contact between the bottom flange of the beam and the column. Daryan [24] used the component method to calculate the rotational stiffness, bending capacity and moment-rotation curves of welded web-cleat connections at high temperatures. The research work summarized above concerns conventional connection types, which lack axial ductility to accommodate the thermal expansion of connected beams at low temperatures, the net shortening caused by the beam catenary action at high temperatures, or the thermal contraction during the cooling stage of the fire.

To improve the high-temperature performance of connections, a novel axially and rotationally

ductile connection with high deformability has been proposed by the authors [25-35]. The configuration of this ductile connection will be introduced in detail later in this paper. A component-based model of the bare-steel ductile connection has been developed; the basic components in the model include fin-plate in bearing, beam web in bearing, bolt in shear, face-plate-semi-cylindrical component, bolt pull-out and column web in compression [27]. On the basis of the bare-steel connection model, a composite ductile connection model has also been established by adding a rebar component [30], which can take into account the pull-out of reinforcing bars and the influence of weld points in the mesh. The bare-steel and composite connection models have been converted into two connection elements following the principles of finite element modelling and incorporated into the software Vulcan [28, 30, 34]. A series of 2-D bare-steel frame models and 3-D composite frame models were built using Vulcan to compare the performance of the ductile connection with other connection types, including the ideally rigid and pinned connections, and the conventional commonly-used types such as end-plate, fin-plate and web-cleat connections [28, 34]. The results show that the axial compressive force of the ductile connection during the early heating stage is significantly lower than that of the other connection types, indicating that the ductile connection can provide high deformability and prevent the buckling of the beam bottom flange during heating. The tensile force of the ductile connection is also lower than that of other connection types when the beam is under catenary action at very high temperatures. The ultimate failure temperature of the ductile connection is higher than that of comparable conventional connection types including end-plate, fin-plate and web-cleat connections, but the differences are not large. The current critical failure mode of the ductile connection is bolt pull-out from the face-plate zone. At very high temperatures, the top bolt row is first pulled out from the bolt holes, and a sequence of pull-out of the remaining bolt rows follows very closely, resulting in the failure of the whole connection. However, when the whole connection fails, the semi-cylindrical section is not completely stretched to flat, so the tensile deformation capacity of the connection is not fully utilized. If the lowest failure modes of the ductile connection can be progressively strengthened, the highest failure temperature of the connection in fire can be achieved.

In this paper, equations for calculating the axial displacements of the top and bottom flanges of the beam end at high temperatures are developed, and the detailed design of the ductile connection is then introduced. A series of Abaqus steel sub-frame models with ductile connections are established

to investigate the influence of the characteristics of the part of the connection between the face-plate and fin-plate parts on the overall connection behaviour. To optimize the bolt pull-out failure, the Abaqus frame models are also used to test some measures including adding a strengthening plate to the face-plate part of the connection, and increasing the connection plate thickness. The elimination of bolt pull-out failure makes another failure mode become critical – the bearing failure of the beam web. To further enhance the failure temperature of the connection, the effect of adding strengthening plates to the part of the beam web in contact with the connection, and improving the material properties of the part of the beam web around the bolt holes on delaying the beam web bearing failure are also studied.

2. Design of the ductile connection

In fire conditions, the deformation of the weakened connected beams causes a complex variation of forces in the structure. During the initial stage of a fire event, heating of a steel down-stand beam causes a free thermal expansion which, if stiffly restrained by surrounding structure, generates very high axial compression. The net compression, hogging bending and shear tend to cause localised shear buckling of the beam web and bottom flange buckling. At very high temperatures, a beam hangs, essentially in catenary tension, between its end connections. When the beam is subsequently cooled from any peak temperature, its contraction will generate high tensile forces between its ends. Therefore, connections at beam ends need to provide sufficient deformation capacity to accommodate the changing beam deformation at high temperatures, so as to enhance the robustness of the whole structure in fire.

2.1 Ductility demands of steel beam in fire

The horizontal movements of the top and bottom flanges at the beam end vary with the change of the beam temperature, as shown in Figure 1 (a) and (b). When the beam temperature is relatively low, usually below 600°C, the thermal expansion of the beam dominates the overall beam deformation, and the movements of the top and bottom of the beam end can be calculated using Equations (1) - (2) derived in the previous paper [25].

$$\Delta_{low-temp,top} = \frac{4}{3}\delta^2_{low-temp} / l + \frac{1}{2}(h\theta_{low-temp} - \alpha lT) \quad (1)$$

$$\Delta_{low-temp,bottom} = \frac{1}{2}(\alpha lT + h\theta_{low-temp}) - \frac{4}{3}\delta^2_{low-temp} / l \quad (2)$$

At high temperatures, the beam loses most of its bending resistance and bears external loads mainly by catenary action. The total strain of the beam section is the sum of the thermal and mechanical strains (Equation (3)). According to force equilibrium, the axial force of the beam under catenary action is a function of external load, beam span and mid-span beam deflection (Equation (4)). Assuming that the shape of the deformed beam is a parabola (Figure 1 (c) and Equation (5)), the elongation of the beam can therefore be calculated by Equation (6). Equation (7) is derived by substituting Equations (4) and (6) into (1). If the movement Δ_C at the centre line of the connection section at high temperature is considered, Equation (8) can be obtained, which can then be used to calculate the movement at the top (Equation (9)) and bottom (Equation (10)) of the beam end. In order to make the calculation results more accurate, the high-temperature stress-strain relationship (Equation (11)) and thermal expansion-temperature relationship (Equation (12)) given by Eurocode 3 [36] can be used.

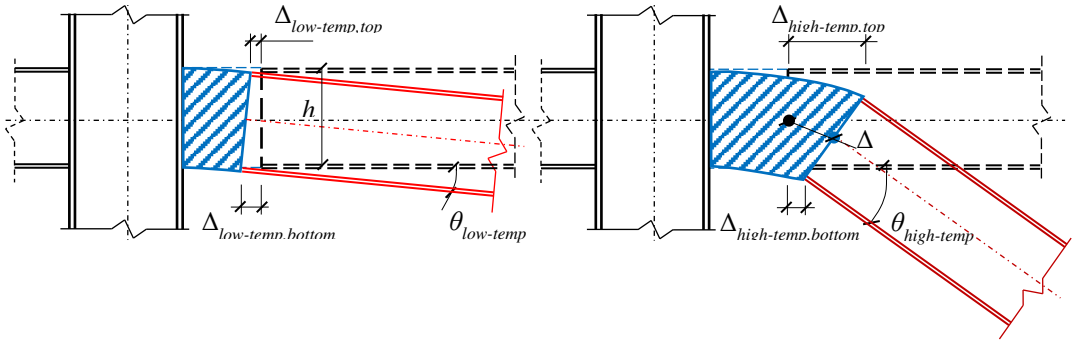

(a) Beam end movement at low temperatures (b) Beam end movement at high temperatures

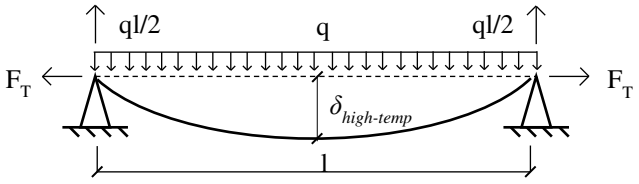

(c) Deformed beam under catenary action

Figure 1. Beam end movement in fire

$$\varepsilon_{total} = \varepsilon_{thermal} + \varepsilon_{mechanical} = \alpha T + \frac{F_T}{AE_T} \tag{3}$$

$$F_T \delta_{high-temp} + \frac{ql}{2} \cdot \frac{l}{4} = \frac{ql}{2} \cdot \frac{l}{2} \quad \Rightarrow \quad F_T = \frac{ql^2}{8\delta_{high-temp}} \tag{4}$$

$$y = -\frac{4\delta_{high-temp}}{l^2} x^2 + \frac{4\delta_{high-temp}}{l} x = \frac{4\delta_{high-temp}}{l^2} \left(xl - x^2 \right) \tag{5}$$

$$\Delta l=\int_0^l \sqrt{1+\left(y'\right)^2}\cdot dx-l=\int_0^l \sqrt{1+\left(\frac{4\delta_{high-temp}}{l^2}(l-2x)\right)^2}\cdot dx-l=\frac{8\delta_{high-temp}^2}{3l} \tag{6}$$

$$\alpha T+\frac{ql^2}{8\delta_{high-temp}AE_T}==\frac{8\delta_{high-temp}{}^2}{3l^2} \tag{7}$$

$$\begin{aligned}&\alpha T+\frac{ql^2}{8\delta_{high-temp}AE_T}+\frac{\Delta_C}{l}==\frac{8\delta_{high-temp}{}^2}{3l^2}\quad\Rightarrow\\&\Delta_C==\frac{8\delta_{high-temp}{}^2}{3l}-\alpha Tl-\frac{ql^3}{8\delta_{high-temp}AE_T}\end{aligned} \tag{8}$$

$$\Delta_{high-temp,top}=\left(\frac{h}{2}-\Delta_C\tan\theta_{high-temp}\right)\cdot\sin\theta_{high-temp}+\frac{\Delta_C}{\cos\theta_{high-temp}} \tag{9}$$

$$\Delta_{high-temp,bottom}=\left(\Delta_C-\frac{h}{2}\tan\theta_{high-temp}\right)\cdot\cos\theta_{high-temp} \tag{10}$$

$$\begin{cases}\text{When}\quad \sigma_T\le f_{pT}\quad \varepsilon_T=\sigma_T/E_T\\ \text{When}\quad f_{pT}\le\sigma_T\le f_{yT}\quad \varepsilon_T=0.02-\sqrt{a^2-\left(\dfrac{\sigma_T-f_{pT}+c}{(b/a)}\right)}\end{cases} \tag{11}$$

$$\begin{cases}\text{When}\quad 20℃\le T<750℃\quad \Delta l/l=1.2\times10^{-5}T+0.4\times10^{-8}T^2-2.416\times10^{-4}\\ \text{When}\quad 750℃\le T<860℃\quad \Delta l/l=1.1\times10^{-2}\\ \text{When}\quad 86℃\le T<1200℃\quad \Delta l/l=12.0\times10^{-5}T-6.2\times10^{-3}\end{cases} \tag{12}$$

2.2 The proposed ductile connection

To prevent connection failures and improve structural robustness in fire a novel connection shown in Figure 2 has been proposed by the authors. This connection can provide additional axial and rotational ductility compared with traditional connection types. The ductile connection can be considered as a replacement for a simple connection and can be used in situations where this type of connection is suitable. It consists of two identical parts, each of which includes a fin-plate bolted to the beam web, a face-plate bolted to the column flange or web, and a semi-cylindrical section between these two parts. These deformed cleats can be fabricated by bending a steel plate. The semi-cylindrical part can ensure the high deformability of the connection by allowing the fin-plate to move towards and away from the face-plate. Therefore, the radius of the semi-cylindrical section is a key dimension of the connection, which should be designed according to the ductility demands of the connected beam under fire conditions (Equations (1), (2), (9) and (10)). Other dimensions of the connection, including the connection thickness and height, the width of the fin-plate and the face-

plate, the bolt spacing, etc., can be designed according to Eurocode 3 [36].

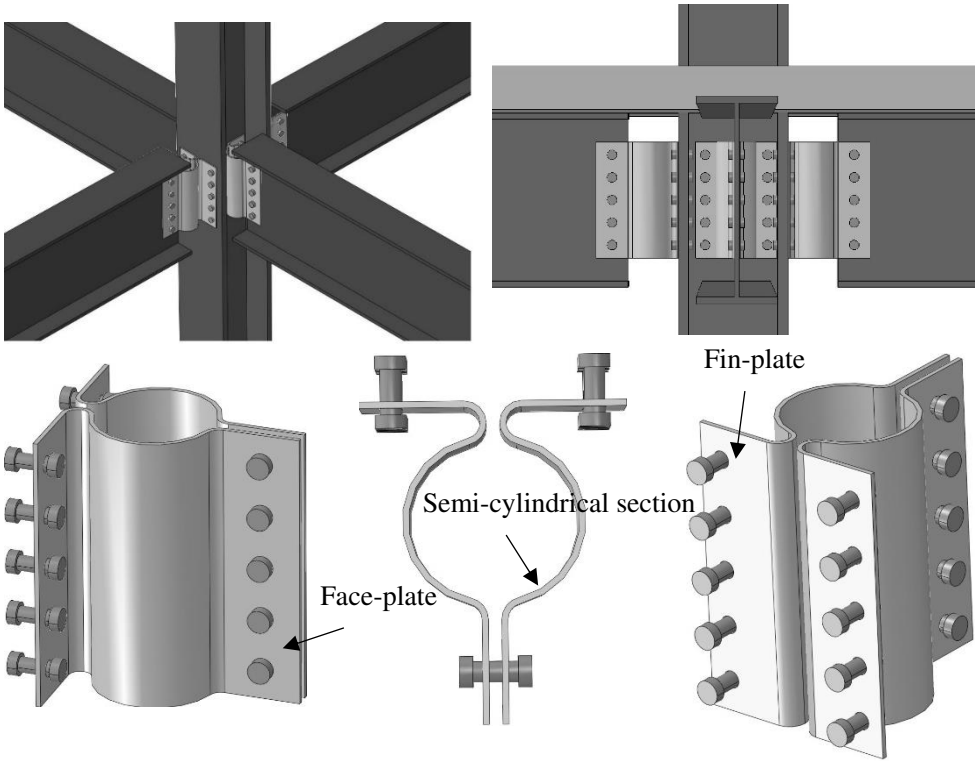

Figure 2. The proposed connection

3. The geometry of the section between the fin-plate and face-plate

3.1 Development of the Abaqus steel frame models

As mentioned previously, the connection part between the fin-plate and the face-plate can provide additional deformability for the ductile connection, and is designed as a semi-cylindrical section. The diameter of the semi-cylindrical section should be determined using Equations (1), (2), (9) and (10). From these equations it can be found that the ductility demands of the beam in tensile and compressive directions are different, implying that the part between the fin-plate and the face-plate should not necessarily be semi-cylindrical, but rather semi-elliptical. In this section, the influence of the geometry of this part on the high-temperature connection behaviour is studied.

The commercial finite element software Abaqus is used to build a series of two-storey three-bay steel frame models with different beam spans and beam sections, as shown in Figure 3. Due to the symmetry of the frame, only half of each model needs to be built. It is further assumed that fire occurs only on the ground floor of the central bay, and the ISO standard fire curve is adopted. The beam temperature is equal to the fire temperature, whereas the temperatures of the connection and the lower column are set to be half of the beam temperature, assuming that they are protected to the

same level. Three beam spans, 6m, 9m and 12m, are selected, and the corresponding beam sections are listed in Table 1. A uniformly distributed line load of 42.64 kN/m is applied to the beams of each frame model, generating a load ratio of 0.4 with respect to simply supported conditions.

Table 1. Dimensions of the Abaqus steel frame models

Span (mm)	Beam section	Load ratio	Connection size				
			Semi-cylindrical (radius: mm)	Semi-elliptical semi-major axis × semi-minor axis (mm × mm)	Fin-plate width × depth (mm × mm)	Face-plate width × depth (mm × mm)	Number of bolt rows
6000	UKB 457×152×82	0.40	55	60 × 45	100 × 290	75 × 290	4
9000	UKB 533×312×151	0.39	75	80 × 65	100 × 360	100 × 360	5
12000	UKB 610×305×238	0.39	125	130 × 115	100 × 430	100 × 430	6

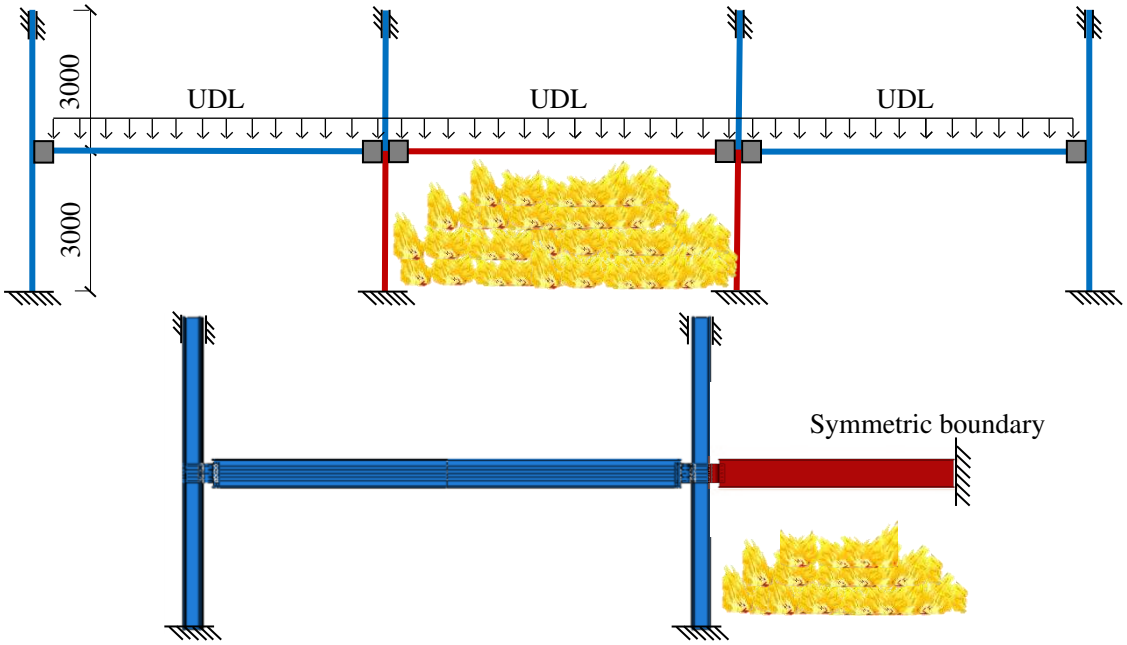

Figure 3. The Abaqus steel frame model

For each beam span, the ductility demands of the beam are calculated first, and then the ductile connections with semi-cylindrical and semi-elliptical configurations are designed according to the range of ductility demand conditions, as shown in Equations (13) (for semi-cylindrical section) and (14) (for semi-elliptical section).The dimensions of the fin-plate and face-plate parts of the connection are designed based on Eurocode 3 [36] as listed in Table 1. The complex contacts

involved in the connection zone of the frame model may lead to numerical singularities if the Abaqus static solver is used, and so the dynamic explicit solver is used to analyse the frame models in this paper, as long as the response of the whole system is quasi-static.

$$\begin{cases} \pi r - 2r \geq \max\left(\Delta_{low-temp,top}, \Delta_{high-temp,top}\right) \\ 2r \geq \max\left(\Delta_{low-temp,bottom}, \Delta_{high-temp,bottom}\right) \end{cases} \tag{13}$$

$$\begin{cases} \dfrac{2\pi b + 4(a-b)}{2} - 2b \geq \max\left(\Delta_{low-temp,top}, \Delta_{high-temp,top}\right) \\ 2b \geq \max\left(\Delta_{low-temp,bottom}, \Delta_{high-temp,bottom}\right) \end{cases} \tag{14}$$

3.2 Validation of the Abaqus steel frame models

The fire tests conducted by Wang [10] on medium-scale restrained steel sub-frames are used to validate the Abaqus simulation method before analysing the results of the Abaqus steel frame models built in the previous section. For this purpose, three tests with different types of connections were selected, including flexible end-plate, flush end-plate and extended end-plate connections. The corresponding Abaqus models for these connections are illustrated in Figure 4. The dimensions of the connections, columns, and beams used in these three tests, along with the material properties obtained from coupon tests at ambient temperature, are listed in Table 2. The elevated temperature stress-strain curves for the different steel materials are in line with the recommendations in Eurocode EN-1993-1-2 [37].

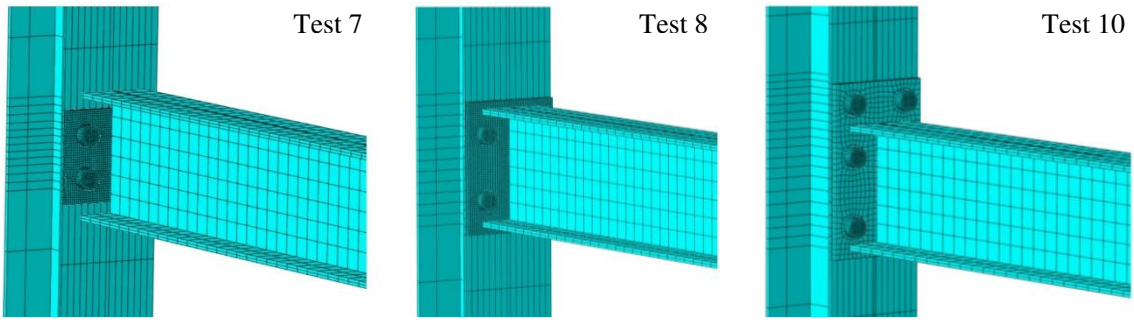

Figure 4. The five corresponding Abaqus models

Table 2. Specimen dimensions and material properties[10]

Test ID	Connection type	Connection size (mm)	Column section	Beam section
Test 7	Flexible end-plate	150 × 130 × 8	UC 152 × 152 ×	UB 178 × 102 × 19
Test 8	Flush end-plate	150 × 200 × 8		
Test 10	Extended end-plate	150 × 250 × 8		

Steel component	Yield stress (MPa)	Ultimate yield stress (MPa)	Young's modulus (kN/mm^2)
Beam & column	350	500	233
Connection	250	450	167
Bolt	640	800	210

The Abaqus models were compared to the test results, as depicted in Figure 5. The main reason for minor discrepancies between the Abaqus results and the test results is the absence of detailed temperature curves for all the different connection components in the fire tests; this information is not given in the paper [10]. As a result, in the Abaqus models, it is assumed that the beam temperature is equal to the fire temperature, and the simple calculation method proposed by Dai and Wang [38] has been used to determine the time-temperature curves for different types of connections. However, it should be noted that this method does not accurately reflect the actual complex temperature distribution and variation observed in the fire tests. Nonetheless, the failure modes captured by the Abaqus models are similar to those observed in the fire tests, as shown in Figure 6. The good agreement between the Abaqus results and the test results indicates that the Abaqus simulation method used in this paper is reasonable.

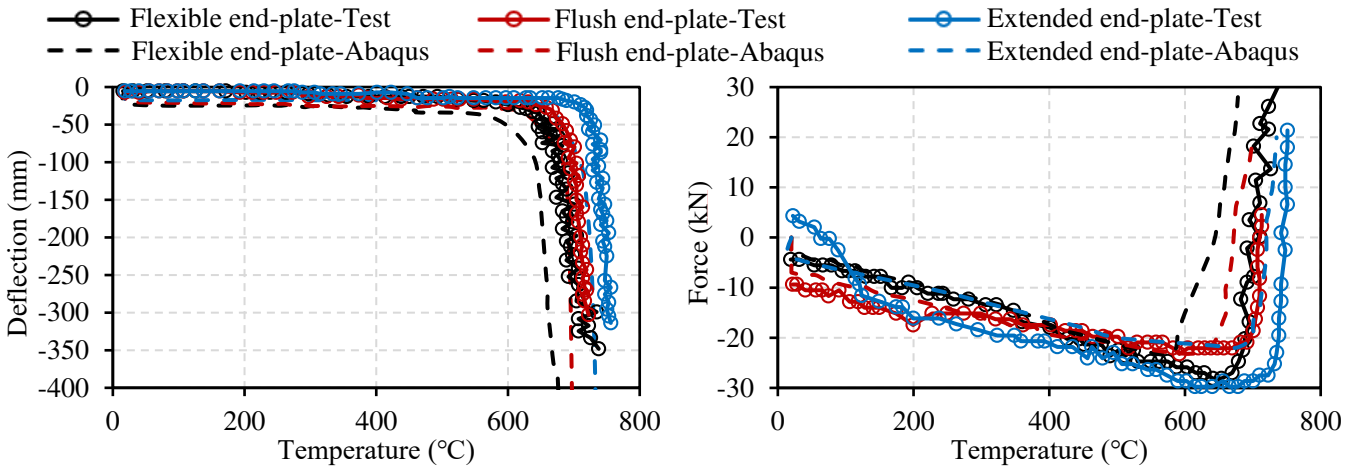

Figure 5. The comparison between Abaqus simulation and test results

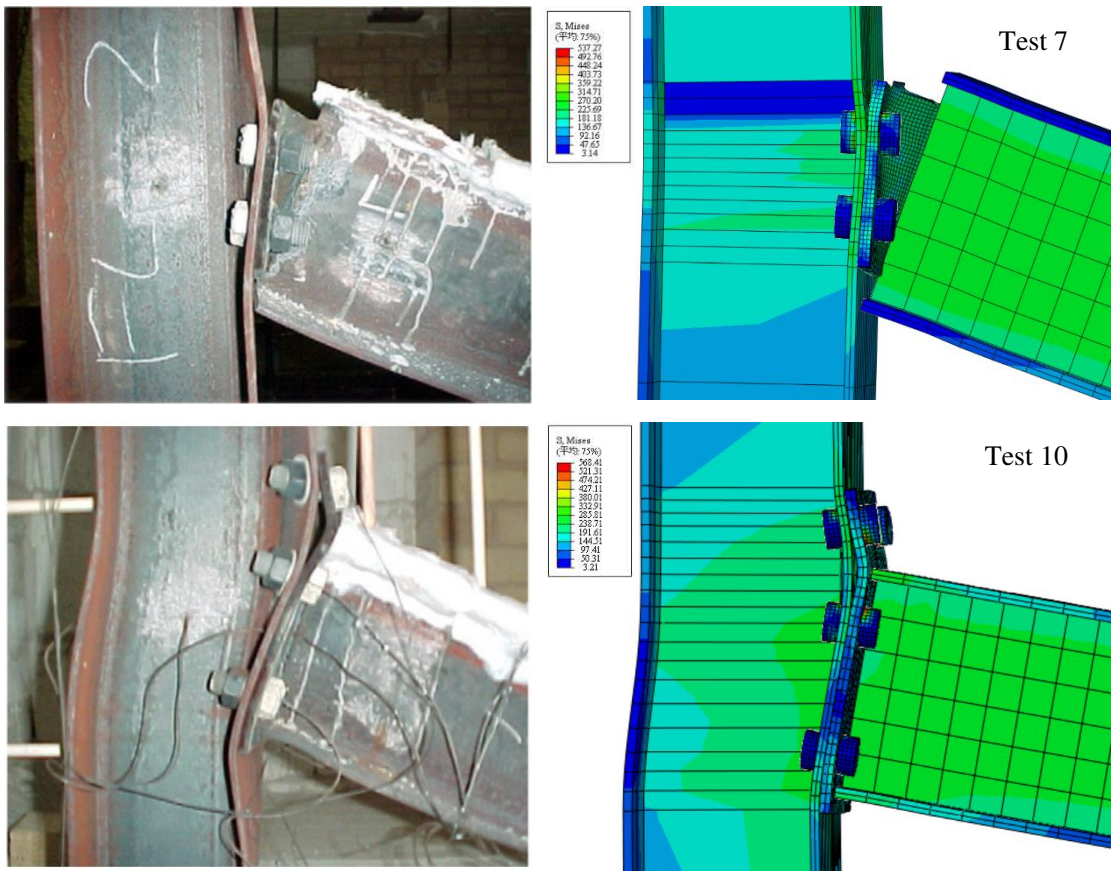

Figure 6. Comparison of failure modes obtained from Abaqus models and tests

3.3 Influence of the geometry of the section between the fin-plate and the face-plate on the connection behaviour

As can be seen from comparison of the results shown in Figure 7 - Figure 9, the geometric shape of the ductile part of the connection has very limited influence on the overall high-temperature performance of the connection. The use of a semi-elliptical section can reduce the compressive force generated in the connection compared with the semi-cylindrical section, but the difference is relatively small. From Figure 7 (c), Figure 8 (c), and Figure 9 (c), it is evident that the axial compressive force in the connection with a semi-elliptical section is slightly lower than that in the connection with a semi-cylindrical section. However, the difference is minimal, with a maximum variation of less than 10%. Both the connection variations exhibit good deformability, as demonstrated by the connection rotation and the axial displacement of the beam end. The compressive axial displacements of the top and bottom flanges of the beam end caused by the beam thermal expansion increase gradually during the initial heating stage when the beam temperature is below 500°C. After this point, the compressive axial displacement of the top flange starts to decrease

and becomes tensile at about 600℃, whereas the compressive axial displacement of the bottom flange continues to increase up to about 700℃. This is because the degradation of material properties dominates the beam behaviour at high temperatures. Taking the model with the beam span of 9m as an example, the maximum tensile displacement of the top flange can exceed 120mm, the maximum compressive displacement of the bottom flange can reach about 60mm, and the maximum connection rotation can reach 0.3rad, which together clearly show the excellent axial and rotational ductility of the new connection. In general, it can be temporarily concluded that the choice of semi-cylindrical or semi-elliptical section can be determined according to the convenience of on-site installation.

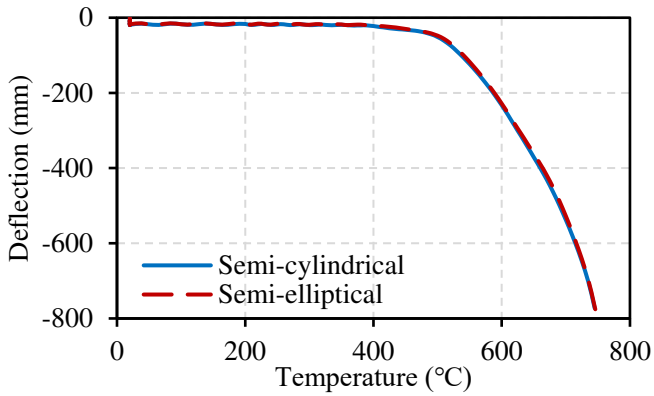

(a) Mid-span deflection of the beam of the central bay

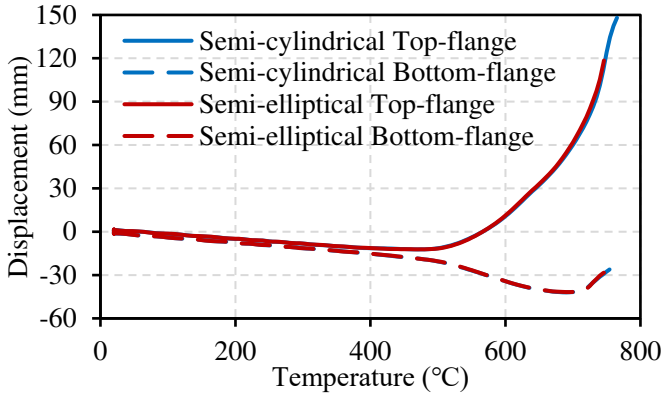

(b) Axial displacement at beam end of the central bay

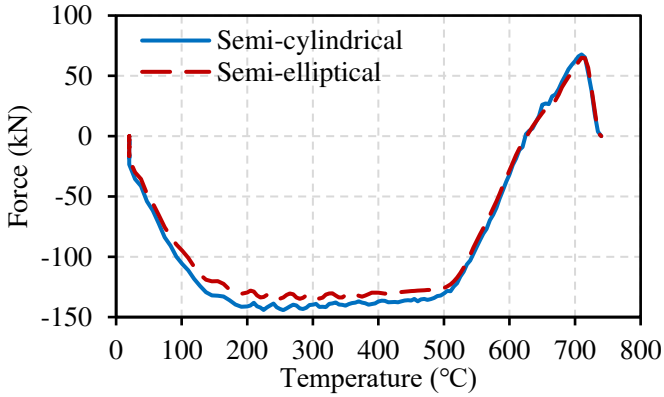

(c) Axial force of the connection of the central bay

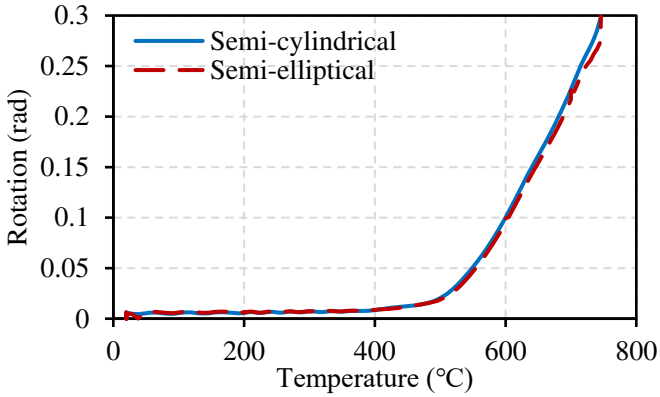

(d) Rotation of the connection of the central bay

Figure 7. Results of the frame models with 6m beam span

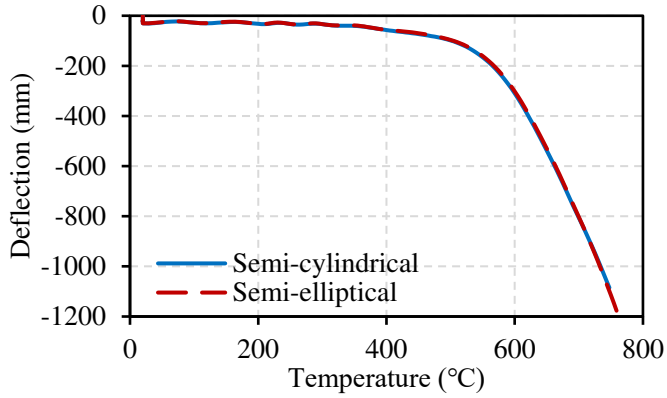

(a) Mid-span deflection of the beam of the central bay

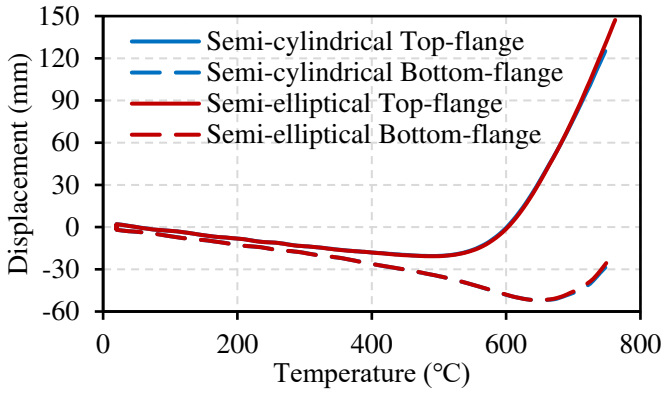

(b) Axial displacement at beam end of the central bay

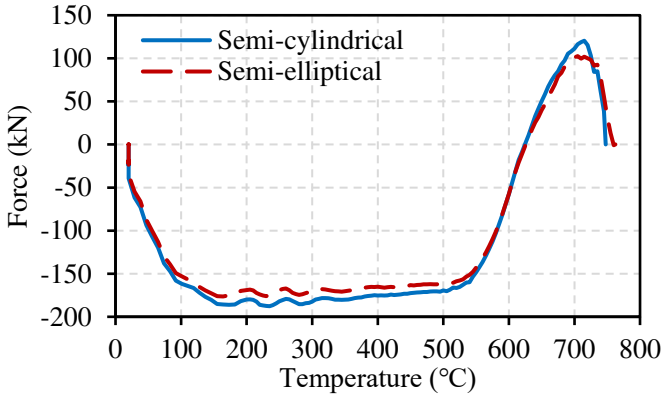

(c) Axial force of the connection of the central bay

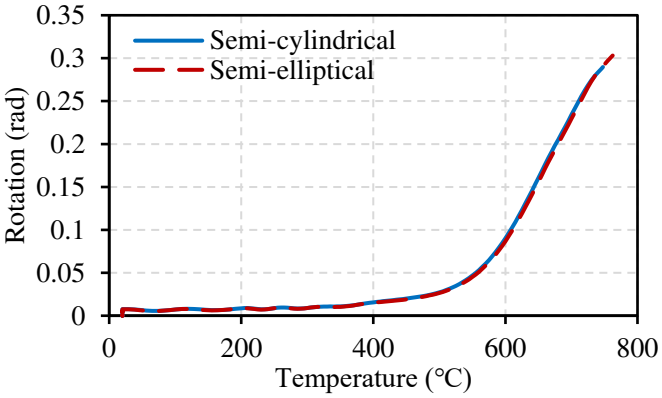

(d) Rotation of the connection of the central bay

Figure 8. Results of the frame models with 9m beam span

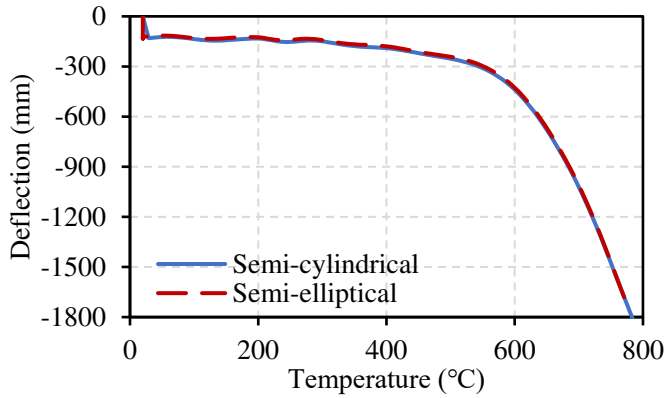

(a) Mid-span deflection of the beam of the central bay

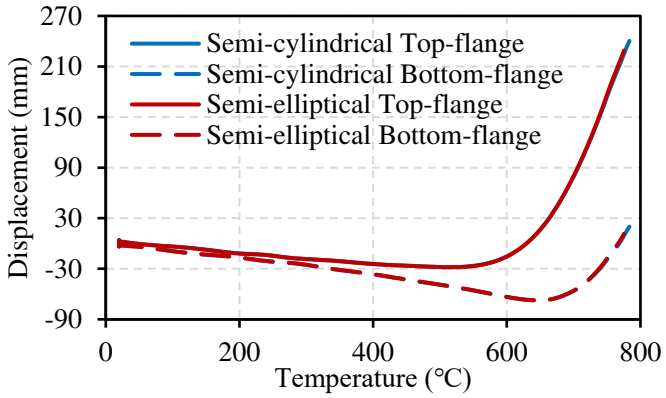

(b) Axial displacement at beam end of the central bay

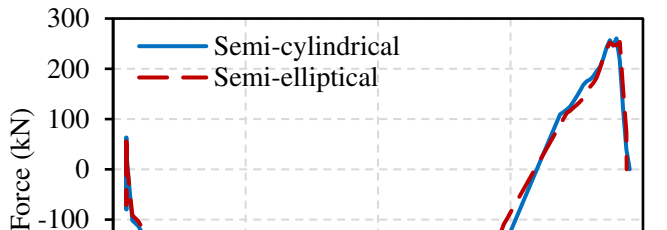

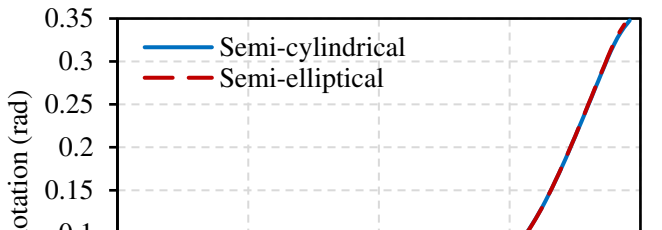

(c) Axial force of the connection of the central bay

(d) Rotation of the connection of the central bay

Figure 9. Results of the frame models with 12m beam span

4. Optimization of failure modes

In previous studies, the fracture temperatures of the ductile connection in fire were seen to be higher than those of conventional connection types, but the differences are not large [7]. The target of the optimization is to progressively strengthen the critical failure modes of the connection to achieve a failure mode which is as close to the tensile failure of the face-plate-semi-cylindrical component as possible.

4.1 Bolt pull-out failure

As mentioned previously, the critical failure mode of an unreinforced ductile connection is bolt pull-out failure from the face-plate zone [28], as shown in Figure 10 (a). At very high temperatures, coinciding with very high rotations, the top bolt row is first pulled out from its bolt holes, and a sequence of pull-out of the remaining bolt rows then follows very closely, resulting in a progressive failure of the whole connection. However, when the whole connection fails, the semi-cylindrical section is not completely stretched flat, so the tensile deformation capacity of the connection has not been fully utilized. To improve the bolt pull-out failure of the connection, the Abaqus steel frame models with 9m beam span introduced in the previous section are used here to test some measures, including adding an additional strengthening plate akin to a column backing plate to the face-plate of the connection (shown in Figure 11 (a)), and increasing the connection plate thickness.

The effect of using strengthening plates to prevent bolt heads from penetrating the face-plate part of the connection is tested first. Two parameters, the thickness and width of the strengthening plate are studied, and the results are shown in Figure 12 and Figure 13. The use of the strengthening plate can effectively prevent the large deformation of the face-plate part, resulting in the critical failure

mode of the connection changing to bearing failure of the beam web, as shown in Figure 10 (b). During the initial heating stage, when thermal expansion dominates the beam deformation, the strengthening plate does not affect the “squeezing” deformation of the connection, and therefore the compressive connection forces of the models with strengthening plates of different thickness (Figure 12 (c)) and width (Figure 13 (c)) are very close to each other. After the connected beam enters the catenary action stage, the strengthening plate reduces the stretching deformation of the connection, resulting in a decrease of beam deflection, connection rotation and axial displacement of the beam end, although the difference is very small. A connection with thicker strengthening plate experiences larger tensile force and less rotation, whereas the influence of the width of the strengthening plate on the connection deformation is negligible. The use of strengthening plate can enhance the ultimate failure temperature of the beam from 745℃ to 753℃.

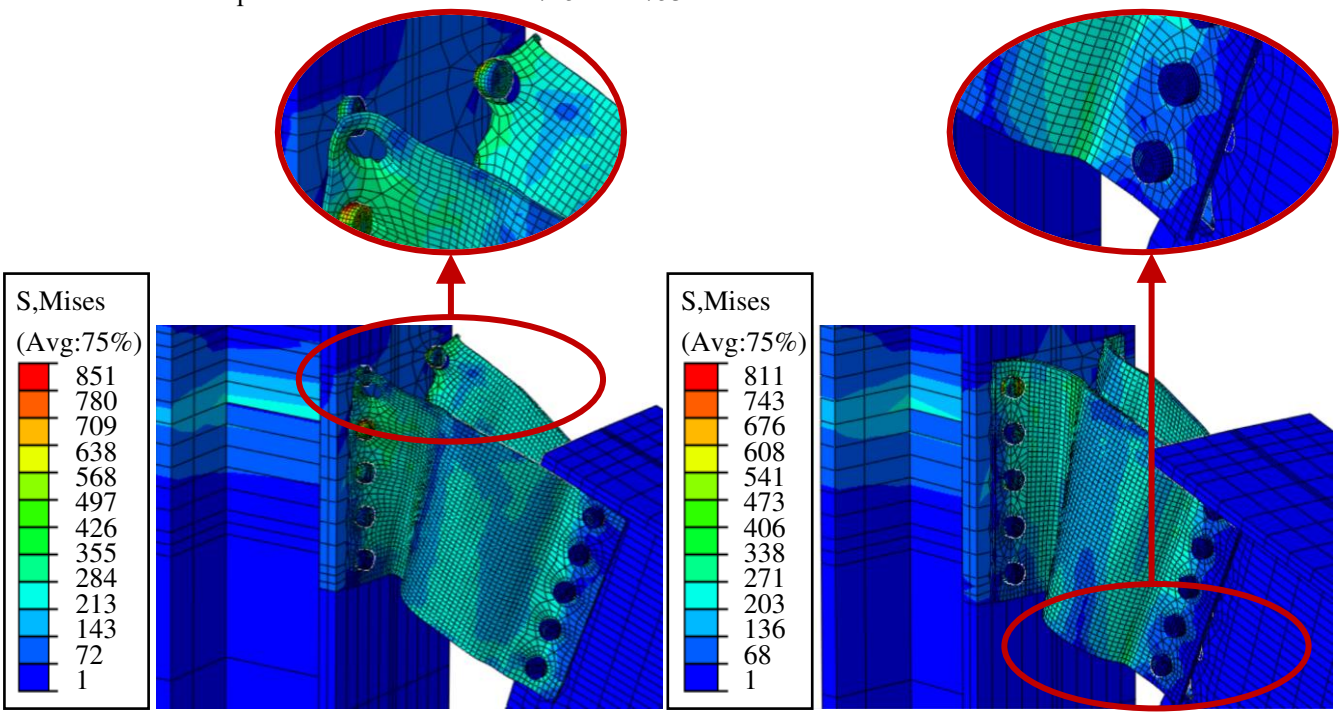

(a) Bolt pull-out failure at the face-plate part (b) Bearing failure of the beam web

Figure 10. Failure modes of the connection

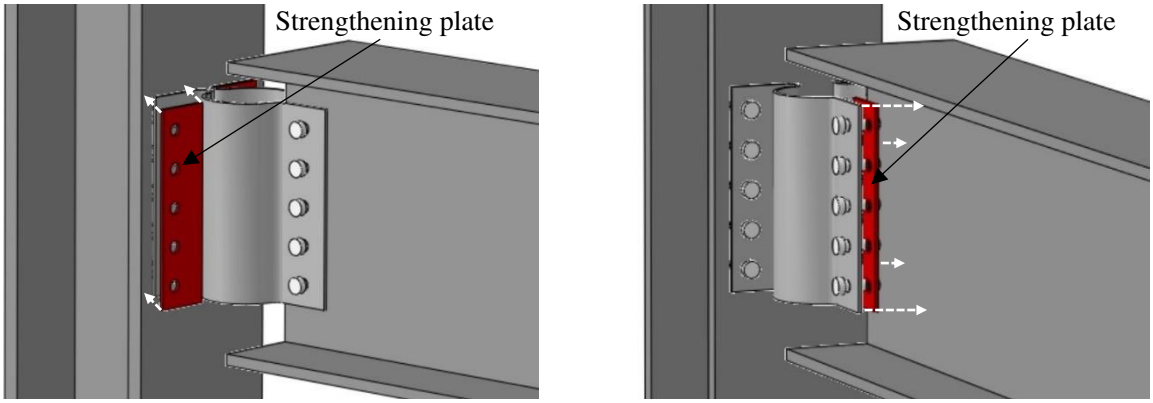

(a) Strengthening plate on the face-plate part

(b) Strengthening plate on the beam web

Figure 11. Strengthening plate

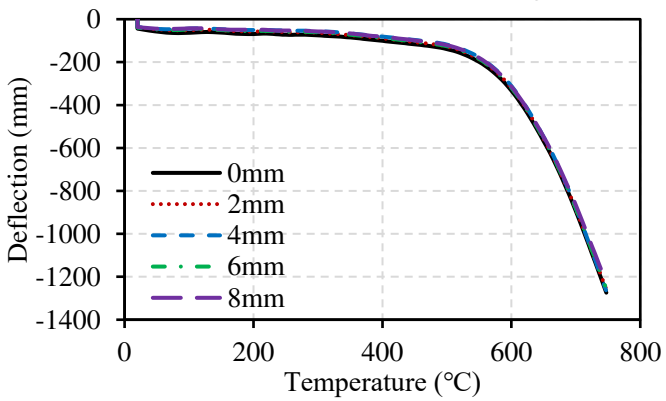

(a) Mid-span deflection of the beam of the central bay

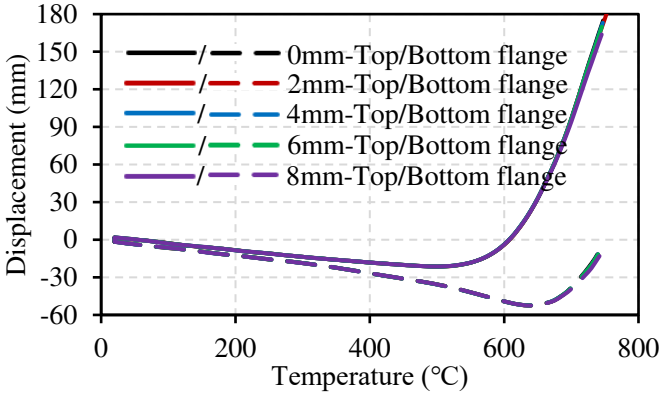

(b) Axial displacement at beam end of the central bay

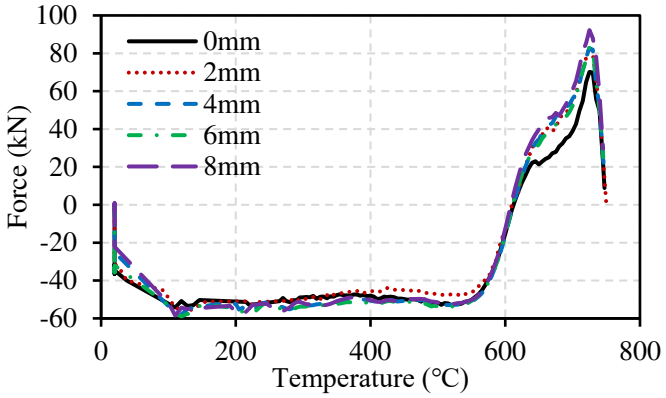

(c) Axial force of the connection of the central bay

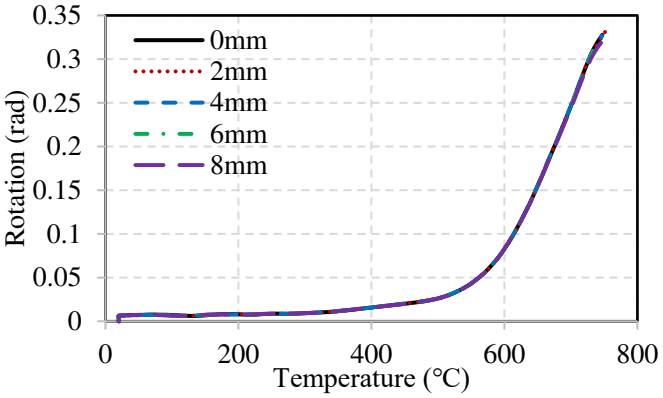

(d) Rotation of the connection of the central bay

Figure 12. Effect of using strengthening plates with different thickness (connection thickness=8mm, strengthening plate width=60mm)

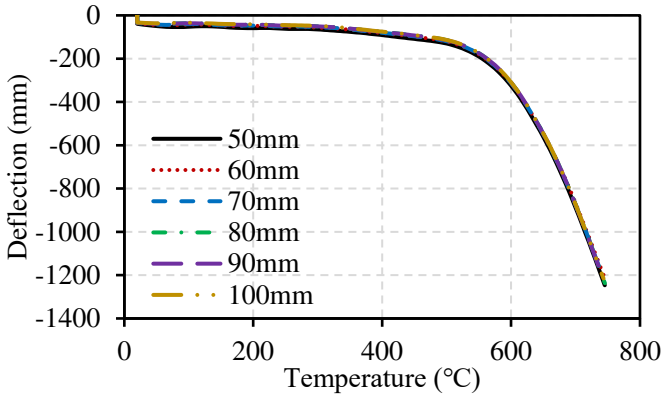

(a) Mid-span deflection of the beam of the central bay

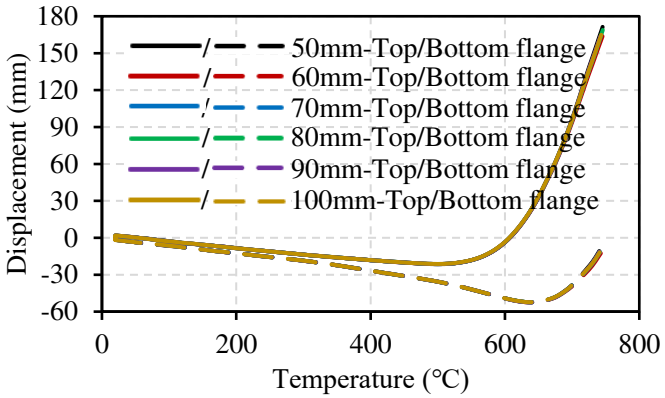

(b) Axial displacement at beam end of the central bay

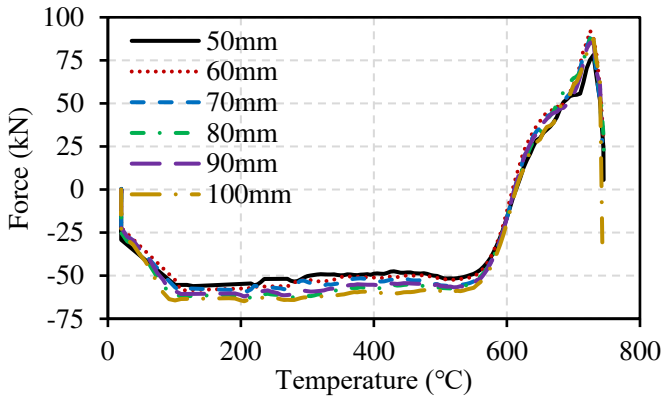

(c) Axial force of the connection of the central bay

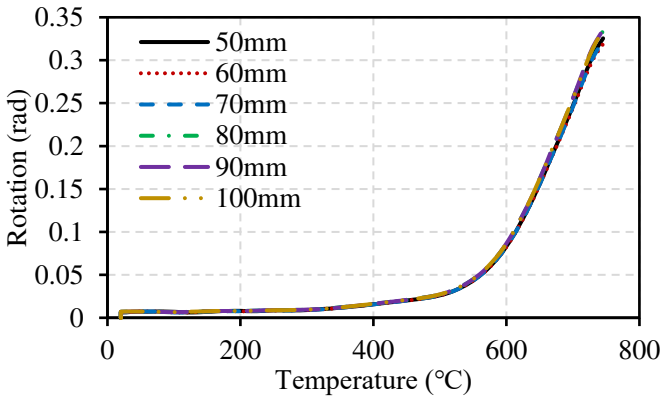

(d) Rotation of the connection of the central bay

Figure 13. Effect of using strengthening plates with different width (connection thickness=8mm, strengthening plate thickness=4mm)

The effect of increase of the connection plate thickness on eliminating bolt pull-out failure has also been examined, and the results are shown in Figure 14. As can be seen from this figure, the deformability of the connection decreases with the increase of the connection plate thickness, which is reflected in the decrease of the beam mid-span deflection (Figure 14 (a)), the axial displacement of the beam end (Figure 14 (b)) and the connection rotation (Figure 14 (d)), as well as a significant increase in the connection axial force (Figure 14 (c)). With the increase of connection plate thickness, the failure mode of the connection also changes from bolt pull-out to beam web bearing failure.

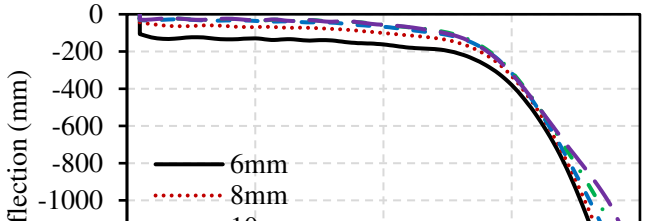

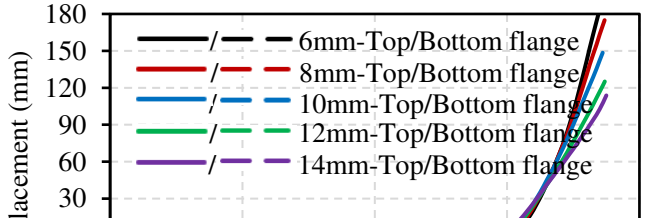

(a) Mid-span deflection of the beam of the central bay

(b) Axial displacement at beam end of the central bay

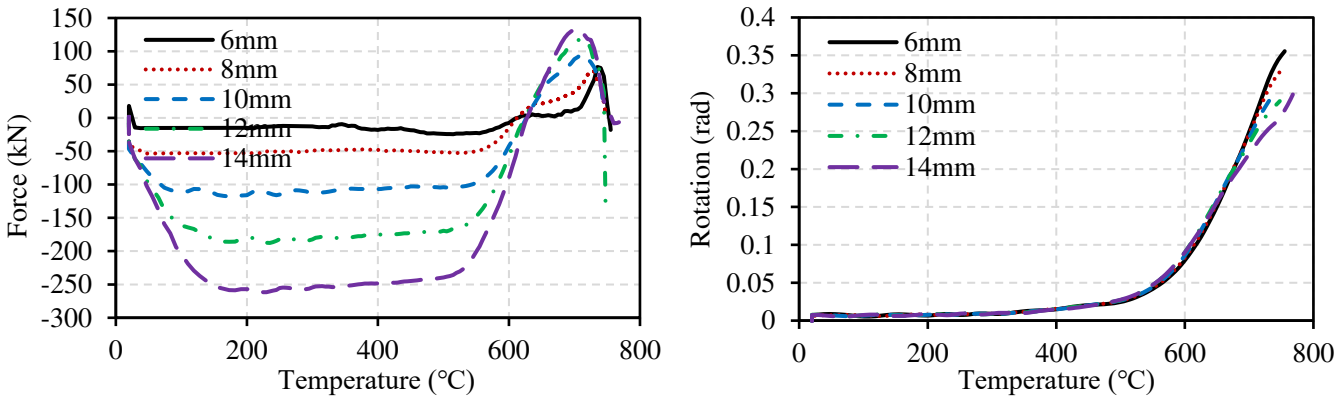

(c) Axial force of the connection of the central bay

(d) Rotation of the connection of the central bay

Figure 14. Effect of increasing connection thickness

4.2 Beam web bearing failure

In the previous section, bolt pull-out failure has been eliminated, resulting in the critical failure mode of the connection changing to bearing failure of the beam web. In this section, the Abaqus sub-frame models with 9m beam span are used to test some measures to optimize beam web bearing failure so that the highest possible failure temperatures of the connection in fire can be achieved. Following the same logic, the strengthening plate used on the face-plate part of the connection might also be used on the beam web to increase the bearing area of the bolt holes, as shown in Figure 11 (b). Strengthening plates of different thickness are welded to the beam web in contact with the fin-plate part of the connection, and the simulation results are shown in Figure 15. It can be seen that the strengthening plate on the beam web does not affect the connection deformation during the initial heating stage. When the temperature rises to a high level and the connection is stretched by the catenary action of the beam, the strengthening plate can effectively reduce the deformation of the bolt holes on the beam web, thus successfully enhancing the ultimate failure temperature of the

connection. The connection with a 10mm thick strengthening plate on the beam web fails at around 812℃, which is a significant increase from the failure temperature of the original connection without optimization (745℃). The thicker the strengthening plate added to the beam web, the higher the failure temperature the connection can reach, indicating that the use of the strengthening plate is an effective method to eliminate the beam web bearing failure, and the ideal failure mode of the connection - the tensile failure of the face-plate-semi-cylindrical component may be achieved.

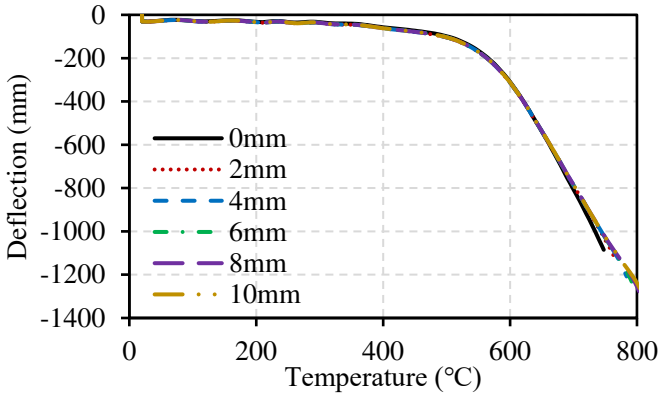

(a) Mid-span deflection of the beam of the central bay

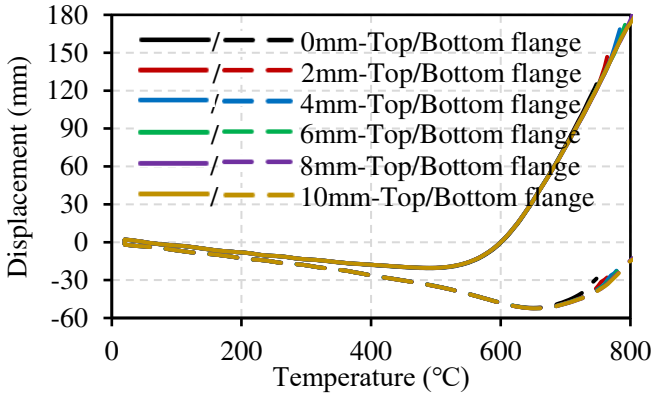

(b) Axial displacement at beam end of the central bay

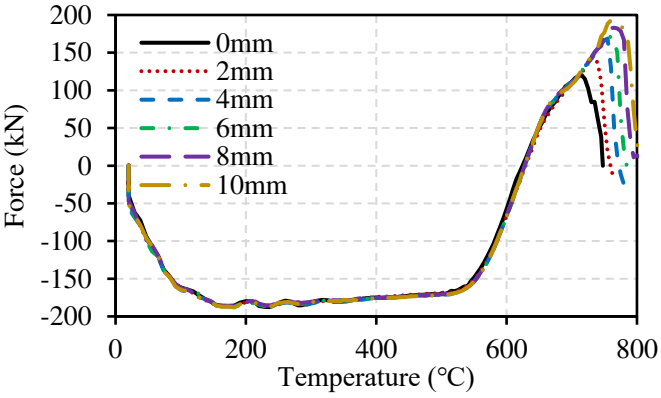

(c) Axial force of the connection of the central bay

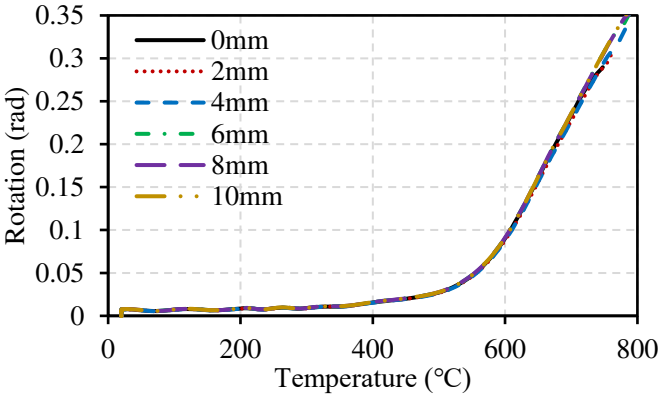

(d) Rotation of the connection of the central bay

Figure 15. Effect of using strengthening plate on beam web

In addition to increasing the bearing area of the beam web, the bearing failure can also be delayed by improving the material properties of the beam web at high temperatures, which can be achieved by using high-strength steel for the added plates or adding fire protection to the connection zone to reduce its temperature. As mentioned previously, the temperature of the central beam in the Abaqus steel frame model is uniform and equal to the fire temperature. In order to test the effect of material properties on the connection performance (or the protection level), the temperature of the beam web

in contact with the fin-plate part is reduced to 90%, 80%, 70%, 60% and 50% of the fire temperature respectively, while the rest of the beam remains equal to the fire temperature. It can be seen from the simulation results shown in Figure 16 that improving the material properties of the beam at high temperatures can effectively delay the occurrence of the beam web bearing failure. When the temperature of part of the beam web in contact with the fin-plate part decreases to 70% of the fire temperature, the ultimate beam temperature at connection failure can reach as high as 1071℃. Considering the cost, adding fire protection to the part of the beam web around bolt holes to reduce its temperature and improve the high-temperature performance of the connection should be a more practical and feasible way, compared with using high-strength steel.

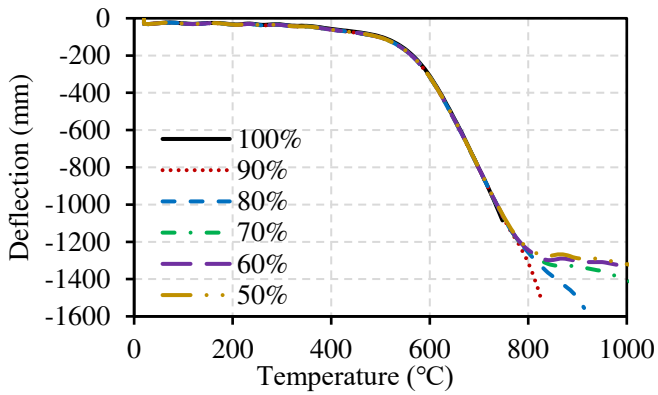

(a) Mid-span deflection of the beam of the central bay

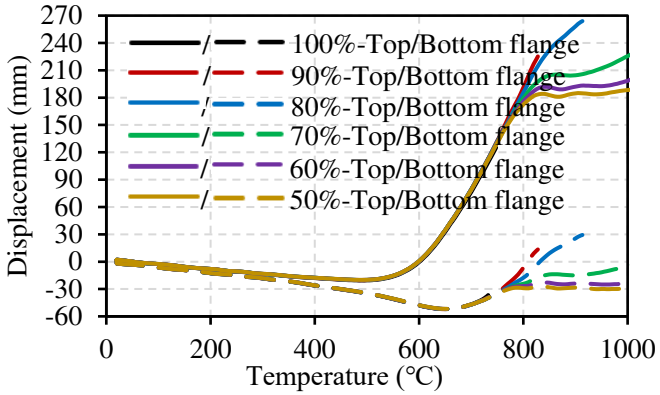

(b) Axial displacement at beam end of the central bay

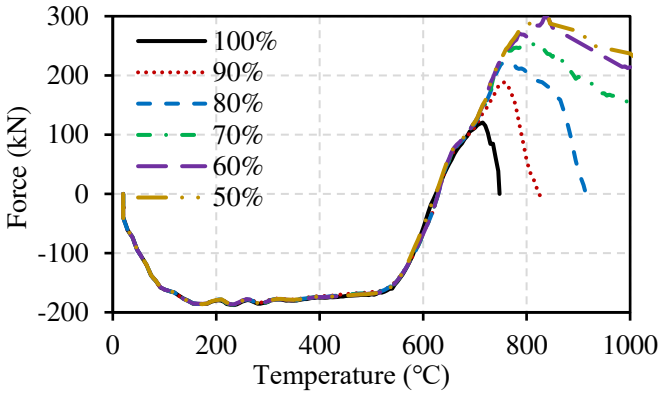

(c) Axial force of the connection of the central bay

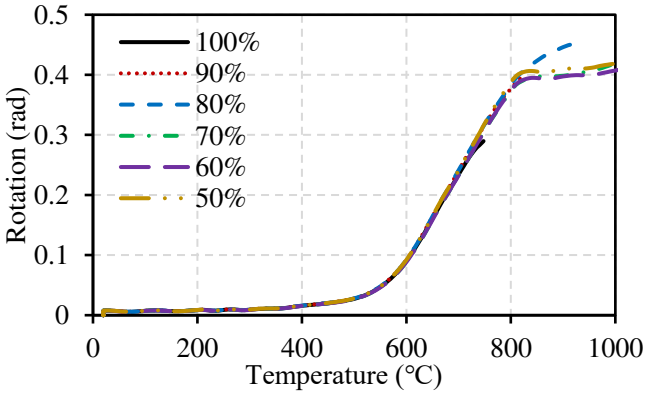

(d) Rotation of the connection of the central bay

Figure 16. Effect of reducing the temperature of the beam web in contact with the fin-plate part

5. Conclusions

Connections are vital to the survival of steel-framed structures in case of fire. A novel ductile connection has been proposed by the authors to improve the high-temperature performance of the

connection. Additionally, this connection holds potential for use in seismic areas, as it can dissipate energy through its deformability, especially where all beam-to-column connections in a building are of this type. However, further research is required to fully investigate this potential. The present study is attempting to make these connections more effective, particularly in the highest-temperature range of a heating curve. Equations to calculate the movements of the top and bottom of the beam end at high temperatures have been proposed first, and then the design of the ductile connection has been introduced.

A series of two-storey three-bay steel sub-frame models with different beam spans and beam sections have been built using Abaqus, to test the influence of the geometry of the connection part between the fin-plate and face-plate parts of the connection on the overall connection performance. It is found that the shape of the middle part of the connection has negligible influence on the high-temperature connection behaviour, as long as its deformability can meet the ductility demands of the beam which can be calculated by the equations proposed in this paper.

Abaqus steel sub-frame models have also been used to test some measures to eliminate bolt pull-out failure at the connection, including adding a strengthening plate to the face-plate part, and increasing the connection plate thickness. The results show that the failure mode of the connection changes from bolt pull-out failure to beam web bearing failure with the increase of either strengthening plate thickness, or the connection plate thickness. Further study will be required to specify general design guidelines for the strengthening plate thickness and the overall connector thickness.

In order to progressively optimize the connection performance, the Abaqus models have also been used to test some measures to delay the beam web bearing failure, including adding strengthening plates to the part of the beam web in contact with the connection, and reducing the temperature of the beam web around the bolt holes. It can be found from the simulation results that the connection with a 10mm thick strengthening plate on the beam web fails at around 812℃, and the ultimate failure temperature of the connection can reach as high as 1071 ℃ when the temperature of the beam web around the bolt holes is reduced to 70% of the fire temperature. It can be therefore concluded that these two methods are very effective in improving the high-temperature performance of the connection.

Acknowledgment

This work was sponsored by Shanghai Pujiang Program (No.22PJ1411500), and National Natural Science Foundation of China (No.52208489, No.51978401). Special thanks to the two students from the research group for their valuable contributions.

Conflict of Interest

On behalf of my co-authors, I would like to submit our original research article entitled "Optimization of failure modes of a ductile connection under fire conditions" to be considered for publication as a research paper in Fire Technology. I confirm that this manuscript has not been published and is not under consideration for publication elsewhere.

The authors declare that they have no potential conflict of interest.

References

[1] T. McAllister, G. Corley, World Trade Center Building performance study: Data collection, preliminary observations, and recommendations, Federal Emergency Management Agency2002.
[2] G.M. Newman, J.T. Robinson, C.G. Bailey, Fire safe design: A new approach to multi-storey steel-framed buildings, Steel Construction Institute2000.
[3] R.G. Gann, W.L. Grosshandler, H.S. Lew, R.W. Bukowski, F. Sadek, F.W. Gayle, J.L. Gross, T.P. McAllister, J.D. Averill, J.R. Lawson, Final Report on the Collapse of World Trade Center Building 7. Federal Building and Fire Safety Investigation of the World Trade Center Disaster (NIST NCSTAR 1A)*** DRAFT for Public Comments, 2008.
[4] K.S. Al-Jabri, The behaviour of steel and composite beam-to-column connections in fire, University of Sheffield, 1999.
[5] H. Yu, I. Burgess, J. Davison, R. Plank, Tying capacity of web cleat connections in fire, Part 1: Test and finite element simulation, Engineering Structures 31(3) (2009) 651-663.
[6] H. Yu, I. Burgess, J. Davison, R. Plank, Experimental investigation of the behaviour of fin plate connections in fire, Journal of Constructional Steel Research 65(3) (2009) 723-736.
[7] H. Yu, I. Burgess, J. Davison, R. Plank, Experimental and numerical investigations of the behavior of flush end plate connections at elevated temperatures, Journal of Structural Engineering 137(1) (2010) 80-87.
[8] Y. Hu, J. Davison, I. Burgess, R. Plank, Experimental study on flexible end plate connections in fire, Proceedings of 5th European Conference on Steel Structures, Graz, Austria, 2008, pp. 1007-1012.
[9] S.-S. Huang, B. Davison, I.W. Burgess, Experiments on reverse-channel connections at elevated temperatures, Engineering structures 49 (2013) 973-982.
[10] Y. Wang, X. Dai, C. Bailey, An experimental study of relative structural fire behaviour and robustness of different types of steel joint in restrained steel frames, Journal of Constructional Steel Research 67(7) (2011) 1149-1163.
[11] Q.-Y. Song, A. Heidarpour, X.-L. Zhao, L.-H. Han, Post-earthquake fire behavior of welded steel I-beam to hollow column connections: An experimental investigation, Thin-Walled Structures 98 (2016)

143-153.
[12] M. Sagiroglu, Experimental evaluation of the post-fire behavior of steel T-component in the beam-to-column connection, Fire safety journal 96 (2018) 153-164.
[13] M. Sarraj, I. Burgess, J. Davison, R. Plank, Finite element modelling of steel fin plate connections in fire, Fire Safety Journal 42(6-7) (2007) 408-415.
[14] M. Sarraj, The behaviour of steel fin plate connections in fire, University of Sheffield, 2007.
[15] H. Yu, I. Burgess, J. Davison, R. Plank, Numerical simulation of bolted steel connections in fire using explicit dynamic analysis, Journal of Constructional Steel Research 64(5) (2008) 515-525.
[16] X. Qiang, F.S. Bijlaard, H. Kolstein, X. Jiang, Behaviour of beam-to-column high strength steel endplate connections under fire conditions–Part 2: Numerical study, Engineering structures 64 (2014) 39-51.
[17] X. Qiang, F.S. Bijlaard, H. Kolstein, X. Jiang, Behaviour of beam-to-column high strength steel endplate connections under fire conditions–Part 1: Experimental study, Engineering Structures 64 (2014) 23-38.
[18] R. Rahnavard, R.J. Thomas, Numerical evaluation of the effects of fire on steel connections; Part 1: Simulation techniques, Case Studies in Thermal Engineering 12 (2018) 445-453.
[19] F. Wald, L.S. Da Silva, D. Moore, T. Lennon, M. Chladna, A. Santiago, M. Beneš, L. Borges, Experimental behaviour of a steel structure under natural fire, Fire Safety Journal 41(7) (2006) 509-522.
[20] X. Qiang, X. Jiang, F.S. Bijlaard, H. Kolstein, Y. Luo, Post-fire behaviour of high strength steel endplate connections—Part 1: Experimental study, Journal of Constructional Steel Research 108 (2015) 82-93.
[21] M. Taib, I. Burgess, A component-based model for fin-plate connections in fire, Journal of Structural Fire Engineering 4(2) (2013) 113-122.
[22] G. Dong, Development of a General-Purpose Component-based Connection Element for Structural Fire Analysis, University of Sheffield, 2016.
[23] S. Lin, Z. Huang, M. Fan, Modelling partial end-plate connections under fire conditions, Journal of Constructional Steel Research 99 (2014) 18-34.
[24] A. Saedi Daryan, The simple model for welded angle connections in fire, International Journal of Steel Structures 17(3) (2017) 1009-1020.
[25] Y. Liu, S.-S. Huang, I. Burgess, Investigation of a steel connection to accommodate ductility demand of beams in fire, Journal of Constructional Steel Research 157 (2019) 182-197.
[26] Y. Liu, S.-S. Huang, I. Burgess, Ductile connections to improve structural robustness in fire, Proceedings of the 6th Applications of Structural Fire Engineering Conference (ASFE'19), Nanyang University of Technology Singapore, 2019.
[27] Y. Liu, S.-S. Huang, I. Burgess, Component-based modelling of a novel ductile steel connection, Engineering Structures 208 (2020) 110320.
[28] Y. Liu, S.-S. Huang, I. Burgess, Performance of a novel ductile connection in steel-framed structures under fire conditions, Journal of Constructional Steel Research 169 (2020) 106034.
[29] Y. Liu, S.-S. Huang, I. Burgess, Investigation of the performance of a novel ductile connection within bare-steel and composite frames in fire, Proceedings of the 11th International Conference on Structures in Fire (SiF2020), The University of Queensland, Asutralia, Queensland, 2020, pp. 662-672.
[30] Y. Liu, S.-S. Huang, I. Burgess, Fire performance of axially ductile connections in composite construction Fire Safety Journal (2021) 103311.
[31] Y. Liu, S.S. Huang, I. Burgess, A numerical study on the structural performance of a ductile

connection under fire conditions, ce/papers 4(2-4) (2021) 1196-1202.
[32] Y. Liu, S.-S. Huang, I. Burgess, Ductile connection to improve the fire performance of bare-steel and composite frames, Journal of Structural Fire Engineering (2021).
[33] Y. Liu, S.-S. Huang, I. Burgess, Performance of ductile connections in 3-D composite frames under fire conditions, Proceedings of the 7th Applications of Structural Fire Engineering (ASFE'21), University of Ljubljana, Ljubljana, 2021, pp. 43-48.
[34] Y. Liu, S.-S. Huang, I. Burgess, Three-dimensional modelling of composite frames with ductile connections in fire, Structures, Elsevier, 2022, pp. 665-677.
[35] Y. Liu, S.-S. Huang, I. Burgess, Numerical investigation of a ductile connection to improve structural robusyness in fire, Proceedings of the 12th International Conference on Structures in Fire (SiF2022), The Hong Kong Polytechnic University, Hong Kong, China, 2022.
[36] CEN, Eurocode 3: Design of steel structures—Part 1-8: Design of joints, (2005).
[37] CEN, Eurocode 3: Design of steel structures - Part 1–2: General rules—Structural fire design. BS EN 1993-1-2: 2005, 2005.
[38] X. Dai, Y. Wang, C. Bailey, A simple method to predict temperatures in steel joints with partial intumescent coating fire protection, Fire technology 46 (2010) 19-35.